

# Actor-Critic Reinforcement Learning with Neural Networks in Continuous Games

Gabriel Leuenberger and Marco A. Wiering

*Institute of Artificial Intelligence and Cognitive Engineering, University of Groningen, The Netherlands*

**Keywords:** Reinforcement Learning, Continuous Actions, Multi-Layer Perceptrons, Computer Games, Actor-Critic Methods.

**Abstract:** Reinforcement learning agents with artificial neural networks have previously been shown to acquire human level dexterity in discrete video game environments where only the current state of the game and a reward are given at each time step. A harder problem than discrete environments is posed by continuous environments where the states, observations, and actions are continuous, which is what this paper focuses on. The algorithm called the Continuous Actor-Critic Learning Automaton (CACLA) is applied to a 2D aerial combat simulation environment, which consists of continuous state and action spaces. The Actor and the Critic both employ multilayer perceptrons. For our game environment it is shown: 1) The exploration of CACLA's action space strongly improves when Gaussian noise is replaced by an Ornstein-Uhlenbeck process. 2) A novel Monte Carlo variant of CACLA is introduced which turns out to be inferior to the original CACLA. 3) From the latter new insights are obtained that lead to a novel algorithm that is a modified version of CACLA. It relies on a third multilayer perceptron to estimate the absolute error of the critic which is used to correct the learning rule of the Actor. The Corrected CACLA is able to outperform the original CACLA algorithm.

## 1 INTRODUCTION

Succeeding in game environments that were originally designed to be played by humans without prior knowledge of the game requires algorithms to be able to autonomously learn to perceive and to act with high dexterity, aimed at maximizing the total reward. Such basic abilities are essential to the construction of animal or human like artificial intelligence. Previous work has demonstrated the applicability of artificial neural networks to games (Tesauro, 1995; Bom et al., 2013; Mnih et al., 2013). Instead of discrete actions that are analogous to button presses we use continuous actions that have to be used to move the control surfaces of an airplane within our 2D aerial combat game environment that involves linear and angular momentum.

The aim of this work is not to engineer algorithms for realistic battles, but to research basic reinforcement learning (RL) algorithms such as the Continuous Actor Critic Learning Automaton (CACLA) (van Hasselt and Wiering, 2007) that learn from scratch in continuous state-action environments. For this the aerial combat environment seems well suited since it provides a larger diversity of challenges than for

instance the pole balancing task that was originally used. For work that is specialized on fully realistic aerial combat see the recently developed Genetic Fuzzy based algorithms that seem to be invincible for human experts (Ernest et al., 2016).

In section 2 we give a short background on reinforcement learning and CACLA. We describe the Ornstein-Uhlenbeck process that can be used to strongly improve the exploration of possible action sequences and a novel Monte Carlo version of CACLA that memorizes the current episode is introduced. We then introduce a novel version of CACLA, Corrected CACLA, that corrects the learning rule of its Actor based on a third MLP that estimates the absolute TD-error. In section 3 we give a description of our aerial combat environment and describe the experimental setup. Section 4 presents the results. The conclusion is given in section 5.

## 2 REINFORCEMENT LEARNING

At every time-step  $t$  the agent receives a state or observation  $s_t$  from its environment. It then outputs an action  $a_t$  that influences the next state of the environ-

ment and obtains a reward  $r_{t+1}$ . The agent starts as a blank slate, not knowing its environment. It should then learn to succeed in its environment by interacting with it over many time steps. The quantity that the agent has to aim at increasing is typically a discounted sum over future rewards called the return  $R_t$  that is defined as follows:

$$R_t := r_{t+1} + \gamma R_{t+1} = \sum_{i=1}^{T-t} \gamma^{i-1} r_{t+i} \quad (1)$$

where  $\gamma \in [0, 1]$  is the discount factor and  $T$  is the time at which the current episode ends. For an extensive introduction to reinforcement learning (RL), see (Sutton and Barto, 1998; Wiering and Van Otterlo, 2012).

One could use unsupervised or semi-supervised learning techniques in order to let the agent construct an internal model of the environment, that could then be used for planning. However this paper focuses on simpler algorithms called model-free RL methods. It is useful to first optimize model-free RL methods in order to show the capabilities that more advanced methods should possess before having learned their model as well as the least amount of dexterity that they should be able to achieve.

In a Markov decision process (MDP) an observation can be interpreted as a state of the environment where the probability distribution over the possible next states depends solely on the current state and action, not on the previous ones. This means that it is sufficient for the agent to choose an action solely based on its current observation. The aerial combat environment that is used in this paper is close to an MDP, therefore we use algorithms that act solely on their current observation or state.

A function that estimates the Return based on the current state is called a Value function:

$$V_t(s) := \mathbf{E}[R_t | s_t = s]$$

If the function additionally takes into account a possible next action, it is called a Q-function:

$$Q_t(s, a) := \mathbf{E}[R_t | s_t = s, a_t = a]$$

Such estimates can be provided by function approximators such as a multilayer perceptron (MLP) that is trained through backpropagation (Rumelhart et al., 1988) to approximate for instance the target  $r_{t+1} + \gamma V_t(s_{t+1})$ , that is a closer approximation of the return. If the Q-function is directly used to evaluate and select the optimal next action, this is called an off-policy algorithm, e.g., Q-learning (Watkins and Dayan, 1992; Mnih et al., 2013).

A function that outputs an action based on the current state is called a policy  $\pi(s)$  and can also be implemented as an MLP. Such parametrized policies

can be used within on-policy algorithms, which facilitates the action selection in continuous action environments among other advantages. The on-policy algorithm used in this paper is an Actor-Critic method (Barto, 1984) that uses both a value function implemented as an MLP, called 'Critic', as well as a policy implemented as a second MLP, called 'Actor'. This algorithm is explained in more detail in the following section.

## 2.1 Continuous ACLA

The Continuous Actor Critic Learning Automaton (CACLA) (van Hasselt and Wiering, 2007) is an Actor-Critic method which is simpler and can be more effective than the Continuous Actor Critic (Prokhorov and Wunsch, 1997). Like other temporal difference learning algorithms CACLA uses  $r_{t+1} + \gamma V_t(s_{t+1})$  in every time step as a target to be approximated by the Critic.

CACLA performs the action that the Actor outputs with the addition of random noise that enables the exploration of deviating actions. In our environment the actions are elements of  $[0, 1]^3$ . The temporal difference error  $\delta_t$  is defined as:

$$\delta_t := r_{t+1} + \gamma V_t(s_{t+1}) - V_t(s_t) \quad (2)$$

In CACLA the Actor  $\pi_t$  is trained during time step  $t + 1$  only if  $\delta_t > 0$ . Once the Critic reached a high accuracy, a positive  $\delta_t$  indicates that the latest performed action  $a_t = \pi_t(s_t) + g_t$  led to a larger value at time  $t + 1$  than was expected at time  $t$  (where  $g_t$  is the noise sampled at time  $t$ ). In a deterministic setting this improvement could be due to the added noise that randomly led to a superior action. Thus the Actor  $\pi_t$  is trained using  $a_t$  as its target to be approximated.

In the original CACLA paper the added noise was white Gaussian noise with a standard deviation of 0.1. In this paper an improved type of noise will be used, called the Ornstein-Uhlenbeck process, that is explained in the following section.

## 2.2 Ornstein-Uhlenbeck Process

In a continuous environment such the one used here, the action sequence produced by an optimal policy is expected to be strongly serially correlated, meaning that actions tend to be similar to their preceding actions. White Gaussian noise however consists of serially uncorrelated samples of the same normal distribution. Adding such noise leads to an inefficient exploration of possible actions as the probability distribution over explored action sequences favours serially uncorrelated sequences rather than more real-

istic, serially correlated sequences. One way to increase the efficiency of exploration is simply to add reverberation to the noise, thus making it serially correlated. White Gaussian noise with reverberation is equivalent to the Ornstein-Uhlenbeck process (Uhlenbeck and Ornstein, 1930), which is the velocity of a Brownian particle with momentum and drag. In discrete time and without the need to incorporate physical quantities it can be written in its simplest form as Gaussian noise with a decay factor  $\kappa \in [0, 1]$  for the reverberation:

$$z_t = \kappa z_{t-1} + g_t \quad (3)$$

The Ornstein-Uhlenbeck process (OUP) has recently been applied in RL algorithms other than CACLA (Lillicrap et al., 2015). In section 4.1 of this paper the performances resulting from the different noise types are compared for CACLA.

### 2.3 Monte Carlo CACLA

A further possibility to improve CACLA’s performance, unrelated to the described exploration noise, is to let it record all of its observations, rewards, and actions within an episode. At the end of an episode, in our case lasting less than 1000 time steps, this recorded data is used to compute the exact returns  $R_t$  for each time step within the episode. The recorded observations can then be used as the input objects in a training set, where the Critic is trained with the target  $R_t$  and if  $R_t - V_t(s_t) > 0$  then the Actor is trained as well with the target  $a_t$ . We call this novel algorithm Monte Carlo (MC) CACLA, and it is based on Monte Carlo (MC) learning as an alternative to temporal difference (TD) learning (Sutton and Barto, 1998).

As later shown in section 4.2 the performance of MC-CACLA is worse than the performance of the original CACLA. We theorize about the possible cause and find the same problem in the original CACLA but to a lesser degree. The new insights led us to a corrected version of CACLA that is described in the following subsection.

### 2.4 Corrected CACLA

Consider a reward  $r_{t+1}$  that is given as a spike in time, i.e., the reward is an outlier compared to the rewards of its adjacent/ambient time steps. In CACLA the Critic takes the current sensory input and outputs  $V_t(s_t)$  that is an approximation of  $r_{t+1} + \gamma V_t(s_{t+1})$ . If the Critic is unable to reach sufficient precision to discriminate this time step with the spike from its ambient time steps then its approximation will be blurred in time. This imprecision can cause the TD-error  $\delta_t$

(equation 2) to be negative in all ambient time steps within the range of the blur around a positive reward spike, or vice versa; to be positive in all ambient time steps within the range of the blur around a negative reward spike as illustrated in Figure 1. In such a case the positive TD-error is not indicative of the previous actions having been better than expected. The original CACLA does not make a distinction and learns the previous actions regardlessly. These might be the very actions that led to the negative reward spike by crashing the airplane. This is a weakness of CACLA that can be corrected to some extent by the following algorithm.

Besides the Actor and the Critic our Corrected CACLA uses a third MLP  $D_t$  with the same inputs, and the same number of hidden neurons. Its only output neuron uses a linear activation function. Like the Critic it is trained at every time-step, but its target to be approximated is  $\log(|\delta_t| + \epsilon)$  with as input the state vector  $s_t$ . The output of this MLP can be interpreted as a prediction and thus as an expected value:

$$D_t(s) = \mathbf{E}[\log(|\delta_t| + \epsilon) | s_t = s]$$

where  $\epsilon$  is a small positive constant that is added to avoid the computation of  $\log(0)$ . We have set the parameter  $\epsilon$  to  $10^{-5}$ . With Jensen’s inequality (Jensen and Valdemar, 1906) a lower bound for the value of the absolute TD-error can be obtained:

$$\mathbf{E}[|\delta_t| | s_t = s] \geq \exp(D_t(s_t)) - \epsilon$$

$D_t$  estimates the logarithm of  $|\delta_t|$  instead of  $|\delta_t|$  itself. This allows for an increased accuracy across a wider range of orders of magnitude and also lowers the impact of the spike on the training of  $D_t$ . The advantage was confirmed by an increased flight performance during preliminary tests.

If  $D_t$  learns to predict a high value of the TD-error for an area of the state-space, this indicates that in this area the absolute TD-error has been repeated on a regular basis and is thus not due to an improved action but due to an inaccuracy of the Critic. Hence we modify CACLA’s learning rule in the following way. In the original CACLA algorithm the Actor is trained on the last action only if  $\delta_t > 0$ . In the Corrected CACLA algorithm the same rule is used, except that this condition is substituted by  $\delta_t > \mathbf{E}[|\delta_t|]$ , where the latter value is the output of the third MLP. Note that this rule only improves the performance around negative reward spikes, thus potentially improving the flight safety. The experiments that were conducted to assess the performance of this novel algorithm are described in the following section.

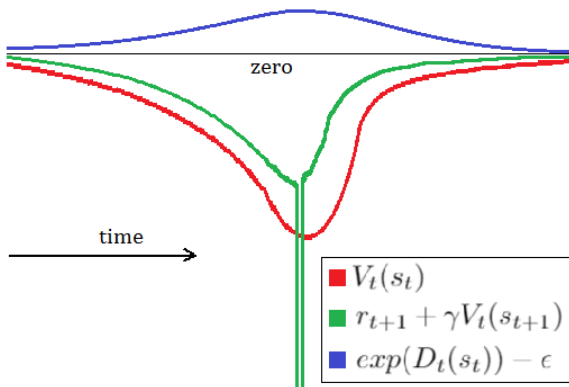


Figure 1: Illustration of the TD-error due to the temporal blur Critic. The TD-error is the difference between the green and the red line. The blue line represents the function used in the Corrected CACLA to estimate the absolute TD-error. The negative reward spike extends far beyond the lower border of the image.

### 3 EXPERIMENTS

#### 3.1 Aerial Combat Environment

In order to compare the different algorithms against each other we use a competitive environment. We only deal with the case where two agents compete against each other with both of them controlling one airplane each, thus there are no other airplanes besides these two. The environment is sequential but divided into episodes. An episode ends either after a player was eliminated or a time limit of 800 time steps has been reached. A player can be eliminated either by crashing into the ground, by crashing into the opponent, or getting hit by five bullets. The starting coordinates and attitude angles of the airplanes are chosen at random, afterwards the game is deterministic until the end of the episode.

The space is two-dimensional where the first dimension represents the altitude and the second dimension is circular. The ground is horizontal and flat with gravity pulling towards it. The altitude has no upper limitation, except for a drop in atmospheric pressure. The airplanes have linear momentum as well as angular momentum that have to be influenced through aerodynamic forces acting on the wings and the control surfaces. If the incoming air hits the wing at an angle larger than 15 degrees then the plane stalls, i.e., it loses lift. This creates the challenge of producing a maximal lateral acceleration without overstepping the stalling angle when flying a curve. Neither the attitude angle nor the angular speed of the plane are directly controlled by the agent. The agent has to learn

to control these through the angle of the elevator and the throttle which are both continuous. Additionally it is required to adapt to the flight dynamics that change with the altitude, since lift and drag are scaled proportionally to the atmospheric pressure that drops exponentially in relation to the altitude. The third output of the agent triggers the fixed forward facing gun that can only give off four consecutive shots before overheating and having to cool down.

The parameters of the flight physics are chosen such that looping is possible at high speeds, spinning is possible at low speeds, and hovering is possible at low altitudes only. The ratio of the size of the airplanes to the circumference of the circular dimension and the drop in pressure are chosen such that the entire game can be viewed comfortably within a  $1000 \times 1000$  pixel window. A sequence of clipped screenshots is shown in Figure 2.

In order to save computational power we do not use the pixels as the sensory input for the agents. For agents that learn directly from pixels see (Koutník et al., 2013; Mnih et al., 2013). The sensory input we used, consists of information that would typically be available to a pilot either through their flight instruments or by direct observation. We list all of the inputs of one agent here. the directions are two-dimensional unit vectors and are calculated from the perspective of one airplane. The scalars are scaled such that their maxima are of the zeroth order of magnitude. The final used inputs are:

- Direction to the horizon and its angular speed
- Altitude and the rate of climb
- Absolute air speed and the acceleration vector
- Distance to the opponent and its rate of change
- Inverse distance to the opponent (apparent size)
- Direction to the opponent and its angular speed
- The orientation of the opponent
- The temperature of the guns

All of the vector components together with the scalars yield a total of 17 continuous inputs. These sensory inputs make the states of the environment fully observable with the exception of the bullets that are invisible to the agents. The environment is thus a partially observable MDP but remains close to a fully observable MDP.

During every time step a reward is given that is proportional to the altitude of the plane and reaches 0.1 at an altitude of 1000 pixels. This reward speeds up the process of learning to fly during the initial stages of training. A reward spike of -25 is given for being eliminated and reward spikes of +5 are given when a bullet hits the opponent.

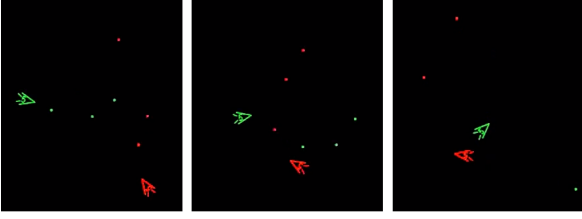


Figure 2: A sequence with two agents on a collision course while attempting to fire bullets at each other. They avoid the collision in the last moment.

The goal of designing this environment was not to construct a fully realistic simulator. For a more complex and fully realistic aerial combat simulation environment see AFSIM (Zeh and Birkmire, 2014) as used in (Ernest et al., 2016).

### 3.2 Experimental Setup

To tune the hyperparameters we performed preliminary experiments. In all of the following experiments each MLP consists of 17 input neurons and 100 hidden neurons with sigmoid activation functions. The output layer of the Critic consists of one neuron with a linear activation function. The output layer of the Actor consists of three neurons with sigmoid activation functions. All of the MLPs are trained with a learning rate of 0.001. The discount factor  $\gamma$  is always set to 0.99. All of the experiments are divided into epochs of which each one consists of 300 episodes of which the last 80 episodes are used for measurements. During these measurements the noise is deactivated and the total reward is averaged over the 80 episodes to produce one data point.

As explained in section 2.2 we run CACLA with the Gaussian noise  $g_t$  for exploration and compare it to a second CACLA where  $g_t$  is replaced by the OUP  $z_t$ . We compare the two algorithms by letting them compete against each other.  $g_t$  does not have the same standard deviation as  $z_t$ . In order to show that the difference in performance is not primarily caused by the differing standard deviations we run a second experiment where  $g_t$  is replaced by  $g'_t$  that is scaled with the factor  $\sqrt[2]{1 - \kappa^2}$  which gives it the same standard deviation as  $z_t$ . The following two equations summarize the relations between the three applied noise signals:

$$z_t := \kappa z_{t-1} + g_t, \quad g'_t := g_t \sqrt[2]{1 - \kappa^2} \quad (4)$$

The reverberation decay factor  $\kappa$  is set to 0.9 because it seemed to perform best in our environment.

The experiments to compare the noise types are run for 40 epochs each. During this time the standard deviation of  $g_t$  is decreased exponentially from 0.2 to 0.02. The experiment is repeated ten times with

different random initializations of the MLP weights, amounting to a total of 120,000 episodes. This entire experiment is conducted once to compare  $z_t$  to  $g_t$  and a second time to compare  $z_t$  to  $g'_t$ . The results of these comparisons are reported in section 4.1.

Since the OUP strongly increases the performance, all of the algorithms used in all of the following experiments employ the OUP with  $\kappa = 0.9$ .

Monte Carlo CACLA (MC-CACLA), as described in section 2.3, is obtained by substituting CACLA's return-approximation  $r_{t+1} + \gamma V_t(s_{t+1})$  with the true return  $R_t$ . The training is then conducted at the end of each episode using the recorded observations and rewards. The competitions between CACLA and MC-CACLA are also 40 epochs long with the noise dropping from a standard deviation of 0.2 down to 0.02. It is also repeated for ten different random initializations of the MLPs. A second experiment is conducted with settings that require more training time but allow for a higher final performance. Each experiment lasts 80 epochs while the standard deviation of the noise is decreased from 0.5 to 0.01. The experiment is repeated for five different random initializations. The results of these experiments are reported in section 4.2.

The Corrected CACLA, as described in section 2.4, is also tested by letting it compete against the original CACLA. Each experiment lasts 80 epochs while the standard deviation of the noise is decreased from 0.5 to 0.01. The experiment is repeated for ten different random initializations. The results of these experiments are reported in section 4.3.

## 4 RESULTS

The results of the experiments are presented as graphs in the next subsections. Each figure represents a competition between two algorithms which influence each other's performance. If for instance the first algorithm always crashes its airplane soon, then the episodes will on average last for a shorter amount of time which will cause the second algorithm to have a lower score as well. The scores of different figures should thus not be directly compared to each other while the scores of the different algorithms within the same figure should be compared.

### 4.1 Ornstein-Uhlenbeck Process

In Figure 3 it can be seen that CACLA with OUP-based exploration significantly outperforms CACLA that uses the original Gaussian exploration. For this Gaussian exploration the signal  $g'_t$  from equation 3.1

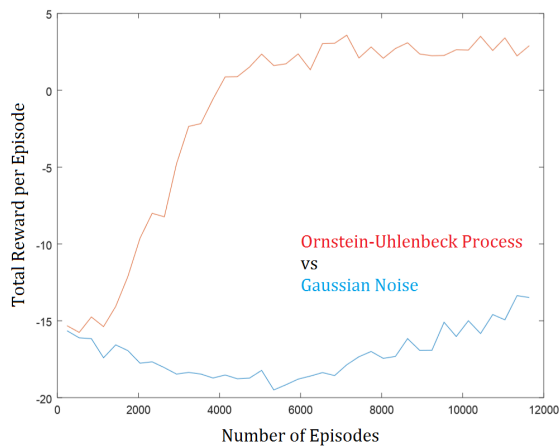


Figure 3: Results of the competition between CACLA with Gaussian exploration ( $g_t'$ ) and CACLA with OUP-based exploration ( $z_t$ ). The graphs are averaged over ten different random initializations. The standard deviation of the noise  $g_t$  was gradually decreased from 0.2 to 0.02.

was used. The signal  $g_t'$  is scaled such that it has the same standard deviation as the signal  $z_t$ . An identical experiment was conducted where the raw  $g_t$  was used instead of  $g_t'$ . The result of this experiment is very similar and thus not reported in this paper.

It can be seen that the total reward of CACLA with Gaussian exploration decreases initially. This could be due to more frequent eliminations through the improving marksmanship of CACLA with OUP-based exploration. By letting experiments run for a longer time it can be observed that CACLA with Gaussian exploration is able to converge to a similar final performance as CACLA with OUP-based exploration. However, CACLA with Gaussian exploration would take an order of magnitude more time to do so.

Due to the strong result, all of the algorithms in the following sections were designed with the OUP-based exploration.

## 4.2 Monte Carlo CACLA

In Figure 4 and Figure 5, it can be seen that the original CACLA strongly outperforms MC-CACLA with the exception of the first 2000 episodes. Since the MC-CACLA uses more memory and uses the accurate Return  $R_t$ , one would intuitively expect MC-CACLA to be superior. One reason of its worse performance is that Monte Carlo learning techniques have a larger variance in their updates than TD-learning algorithms. Another reason could be the spiking rewards that produce a Return that locally resembles a step-function over time. The Critic, approximating this stepping Return, might not be sufficiently precise to discriminate between the surround-

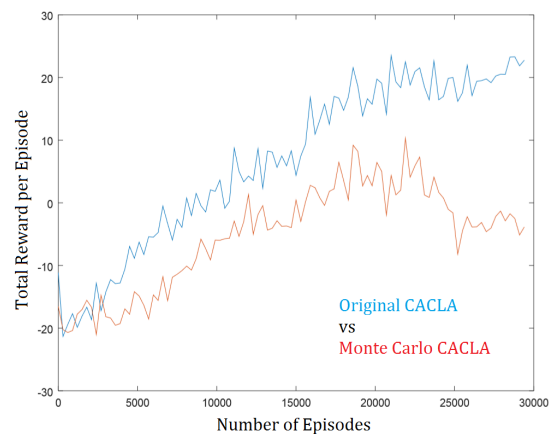


Figure 4: Results of the competition between the Monte Carlo version of CACLA and the original CACLA. The graphs are averaged over five different random initializations. The standard deviation of the noise  $g_t$  was gradually decreased from 0.5 to 0.01.

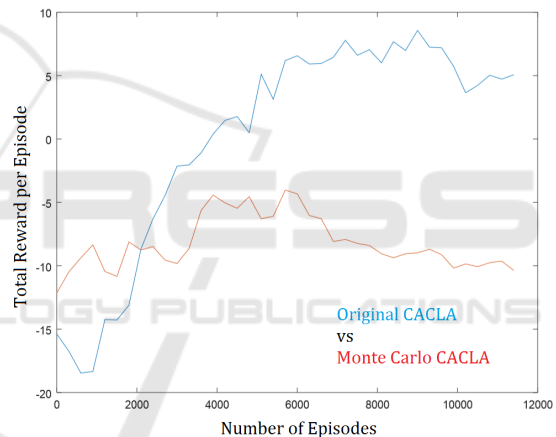


Figure 5: Results of the competition between the Monte Carlo version of CACLA and the original CACLA. The graphs are averaged over ten different random initializations. The standard deviation of the noise  $g_t$  was gradually decreased from 0.2 to 0.02.

ing time steps before and after the reward spike. This would lead to positive or negative differences between the Value and the Return. This would then disturb the Actor's learning rule that relies on the difference  $R_t - V_t(s_t)$ . This problem of the algorithm was then looked for in the original CACLA as well. The problem was found to be theoretically possible in the original CACLA (described in section 2.4), but in a more benign way, the deviation of the Critic around a spike would be smaller in the original CACLA. In section 2.4 a possible solution to this problem was described. The following section presents the results of this solution.

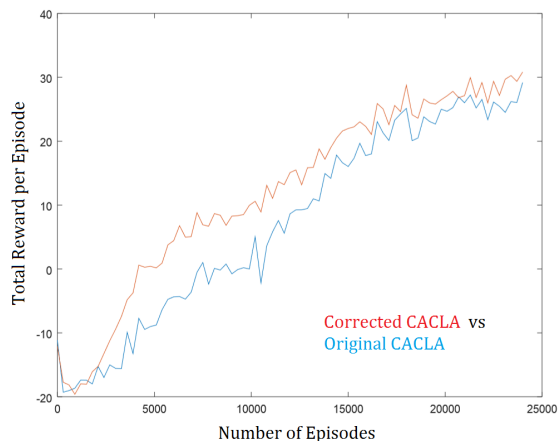


Figure 6: Results of the competition between the Corrected CACLA and the original CACLA algorithm. The graphs are averaged over ten different random initializations. The standard deviation of the noise  $g_t$  was gradually decreased from 0.5 to 0.01.

### 4.3 Corrected CACLA

In Figure 6, it can be seen that the Corrected CACLA on average outperforms the original CACLA. The averages of the total rewards from the first until the last episode were compared. The Corrected CACLA algorithm performed better for ten out of ten random initializations which resulted in a p-value of  $2^{-10}$ . The strongest difference in performance is between the 5000th and the 10,000th episode. Towards the end of the graph the two algorithms converge towards the same strategy and the same performance. The Corrected CACLA algorithm is constructed such that it has an advantage when there are negative reward spikes as explained in section 2.4. This advantage is confirmed by these results. Later, once the agents learned to increase their flight safety such that there are less negative reward spikes, the Corrected CACLA loses its advantage. This advantage might prevail in a different environment where the negative reward spikes do not disappear over time.

## 5 CONCLUSIONS

All of the algorithms were tested by competing in our aerial combat environment. Our results show that substituting the original Gaussian noise in CACLA with the OUP leads to a strongly improved exploration of actions and better performance of the algorithm. This improvement is to be expected in environments where the optimal action sequences are temporally correlated, which is typical for continuous environments. The results also showed that MC-CACLA performs

worse than the original CACLA algorithm. More work on a Monte Carlo version of CACLA would need to be done. One possible cause of the poor performance is that the temporal inaccuracy of the Critic disturbs the learning rule of the Actor. The same problem was found in the original CACLA but to a much lesser degree. This problem appears when spiking rewards are given. We solved this problem in CACLA by adding a third MLP that is used to predict the logarithm of the absolute error of the Critic. The learning rule of the Actor was then adapted such that it is trained only when the TD-error is larger than the estimated absolute error of the Critic. This algorithm was described in detail in section 2.4. The results show that this approach can indeed improve the performance over the original CACLA algorithm. This result is remarkable because the Actor in the Corrected CACLA is trained less often than in the original CACLA. However our Corrected CACLA likely only has an advantage in environments where negative reward spikes occur.

In future research a similar algorithm could be developed that also improves CACLA's performance when there are mostly positive reward spikes. Furthermore, extending these algorithms by a learnable model that is used to plan ahead at multiple temporal resolutions could strongly improve the final performance of agents in this aerial combat environment. This is left as future research.

## REFERENCES

- Barto, A. (1984). Neuron-like adaptive elements that can solve difficult learning control-problems. *Behavioural Processes*, 9(1).
- Bom, L., Henken, R., and Wiering, M. (2013). Reinforcement learning to train Ms. Pac-Man using higher-order action-relative inputs. In *Proceedings of IEEE International Symposium on Adaptive Dynamic Programming and Reinforcement Learning : ADPRL*.
- Ernest, N., Carroll, D., Schumacher, C., Clark, M., Cohen, K., and Lee, G. (2016). Genetic fuzzy based artificial intelligence for unmanned combat aerial vehicle control in simulated air combat missions. *J Def Manag*, 6(144):2167–0374.
- Jensen, J. and Valdemar, L. (1906). Sur les fonctions convexes et les inégalités entre les valeurs moyennes. *Acta mathematica*, 30(1):175–193.
- Koutník, J., Cuccu, G., Schmidhuber, J., and Gomez, F. (2013). Evolving large-scale neural networks for vision-based reinforcement learning. In *Proceedings of the 15th annual conference on Genetic and evolutionary computation*, pages 1061–1068. ACM.
- Lillicrap, T., Hunt, J., Pritzel, A., Heess, N., Erez, T., Tassa, Y., Silver, D., and Wierstra, D. (2015). Continu-

- ous control with deep reinforcement learning. *arXiv preprint arXiv:1509.02971*.
- Mnih, V., Kavukcuoglu, K., Silver, D., Graves, A., Antonoglou, I., Wierstra, D., and Riedmiller, M. (2013). Playing atari with deep reinforcement learning. *arXiv preprint arXiv:1312.5602*.
- Prokhorov, D. and Wunsch, D. (1997). Adaptive critic designs. *IEEE transactions on Neural Networks*, 8(5):997–1007.
- Rumelhart, D., Hinton, G., and Williams, R. (1988). Learning representations by back-propagating errors. *Cognitive modeling*, 5(3):1.
- Sutton, R. and Barto, A. (1998). *Reinforcement learning: An introduction*, volume 1. MIT press Cambridge.
- Tesauro, G. (1995). Temporal difference learning and TD-gammon. *Communications of the ACM*, 38(3):58–68.
- Uhlenbeck, G. and Ornstein, L. (1930). On the theory of the brownian motion. *Physical review*, 36(5):823.
- van Hasselt, H. and Wiering, M. (2007). Reinforcement learning in continuous action spaces. In *Approximate Dynamic Programming and Reinforcement Learning, 2007. ADPRL 2007. IEEE International Symposium on*, pages 272–279.
- Watkins, C. and Dayan, P. (1992). Q-learning. *Machine learning*, 8(3):279–292.
- Wiering, M. and Van Otterlo, M. (2012). *Reinforcement Learning State-of-the-Art*, volume 12. Springer.
- Zeh, J. and Birkmire, B. (2014). Advanced framework for simulation, integration and modeling (AFSIM) version 1.8 overview. *Wright Patterson Air Force Base, OH: Air Force Research Laboratory, Aerospace Systems*.